Electronics and Electrical Engineering

AIMS Electronics and Electrical Engineering, 8(1): 146–164.
DOI: 10.3934/electreng.2024006
Received: 22 December 2023
Revised: 04 March 2024
Accepted: 11 March 2024
Published: 22 March 2024

http://www.aimspress.com/journal/ElectrEng

Research article

A hybrid IDM using wavelet transform for a synchronous generator-based RES with zero non-detection zone

Mamun Mishra* and Bibhuti Bhusan Pati

Department of Electrical Engineering, Veer Surendra Sai University of Technology, Burla, India

*** Correspondence:** Email: mmishra_ee@vssut.ac.in.

Abstract: Increased use of renewable energy sources in distribution grids has led to the growing concern over unintentional islanding. Among the available islanding detection methods, the passive methods have larger non-detection zones and are susceptible to system faults. However, they have no effect on power quality like active methods. We present a hybrid method for the islanding detection of synchronous generator-based renewable energy sources. Here, the larger non-detection zone issue of the passive islanding detection method was reduced by combining it with a wavelet transform. The rate of change of a voltage unbalanced factor was computed from the sequence components of the renewable energy source terminal voltage. Then, the factor was analyzed using a wavelet transform, and a threshold for the factor was found. The robustness of the method was tested for several islanding as well as non-islanding situations. The efficacy of the method was also tested in multi-source test systems. From the analysis, it was observed that the proposed method was fast, reliable, and had a zero non-detection zone.

Keywords: microgrid; renewable energy source; islanding detection method; non-detection zone; wavelet transform; voltage unbalance

1. Introduction

Grid integrated renewable energy sources (RESs) can operate in two modes. One is the grid-connected mode and the other is the islanded mode. In islanded mode, the RES continues to energize its nearby areas despite being disconnected from the main utility grid. Due to its intermittent

nature, of the RES and the power electronic interfaces, the voltage and the frequency will be affected in the islanded mode of operation. Thus, fast detection of utility disconnection is very much required. According to the IEEE 1547 standard for RES integration, the island formation should be detected within 2 sec of its occurrence [1]. All the available islanding detection methods (IDMs) can be classified as passive detection methods (PDMs), active detection methods (ADMs), remote detection methods (RDMs), hybrid detection methods (HDMs), signal processing-based detection methods (SPDMs), and intelligence-based detection methods (IBDMs).

The PDMs monitor the parameters at the terminals of RESs or at the point of common coupling (PCC) and compare them with a set threshold. Many studies on PDMs have been conducted and reported [2–5]. The PDM has no effect on power quality. However, the major issues with PDMs are large non-detection zones and threshold settings [2]. Many PDMs mostly fail to detect when there is a close match between power generation and load consumption in the islanded area. Again, if the threshold is set too high, many islanding condition may go undetected, and if it is set too low, it may lead to nuisance tripping causing reliability issues. A number of passive methods such as over/under voltage/ frequency [2–4], rate of change of frequency (ROCOF) [2,3], ROCOF over power [4], total harmonic distortion [5], phase jump detection [5], and voltage vector shift [5] are developed to detect the islanding phenomenon. In [6], two PDMs based on ROCOF and voltage surge (VS) relay performances are analyzed and compared for synchronous generator-based RES. It is found that, the ROCOF relay is more susceptible to false operation than VS relay.

In ADMs, a known disturbance is added to the system parameters at the RES terminal and the effect is analyzed for assessing utility disconnection. Mostly, the ADMs are applicable to power electronic interfaced RES [5]. Unlike PDMs, ADMs have a small non-detection zone and there is no need of threshold setting. However, these methods affect the power quality and are not applicable to multi-source systems [5]. Several ADMs, like active frequency drift [5], sliding mode frequency shift [7], Sandia frequency shift [8], and PDMs [9], have been implemented.

The RDMs are positioned on the utility side. These methods have a zero non-detection zone, negligible impact on power quality, and are applicable to multi-source systems. However, a huge investment is required for the implementation of RDMs due to the requirement of a communication medium. In [10], the RDM is based on local measurements. Here, a large impedance is inserted on the low voltage side of the grid. An intelligent hybrid automatic transfer switch (HATS) is employed as the microgrid control switch, which is embedded with an IDM agent. Then, the current magnitude difference on the inserted impedance and the HATS is used as an indicator of utility disconnection. The performance of the method is not tested for non-islanding conditions such as faults and load switching.

In HDM, the above conventional methods are combined to overcome the drawbacks of individual methods. In [11], the voltage unbalance parameter is used as a passive parameter, and voltage phase angle (VPA) is used as an active parameter for a new hybrid method. For the implementation of the VPA technique, the difference between the instant and nominal VPA is added to the abc - to - dqo block. Though the method does not have a non-detection zone, there is some effect on power quality. In [12], PDM and RDM are combined and a control strategy in the autonomous mode of operation of the system after isolation is presented. However, the method is not tested with faults, load switchings, or multi-source systems.

In SPDMs and IBDMs, the conventional methods are combined with signal processing techniques and intelligent or soft-computing techniques [5,13,14]. In [17], both phase voltages and

negative sequence voltage is analyzed with a Wavelet transform. Both methods are found to be able to detect the islanding condition fast, even at a zero-power mismatch with low sampling frequency. However, the analysis of multiple parameters leads to longer computation time. In [18], the wavelet coefficients of phase voltages are found. Then, the energy content in the detailed coefficients of each phase is calculated and is compared with a threshold for islanding detection. However, the method is not tested for non-islanding conditions. In [19], one of the wavelet coefficients of PCC phase voltage is used for islanding detection even at zero power mismatch. Again in [20], two factors using the wavelet coefficients of PCC voltage are found for islanding detection. The method is found to operate even for exact power balance conditions. However, both methods are not implemented for multi-source system and for non-islanding scenarios. In [21,22], instead of voltage signal, current signal is analyzed using a wavelet transform, and standard deviations of the wavelet coefficients are utilized for islanding detection with a defined threshold. Many IBDM are also reported in [23]. These methods have numerous advantages like zero non-detection zone, no effect on power quality, and high reliability but with with some drawbacks like complex system structure, longer computation time due to increased usage of data, and algorithms.

After a detailed study of available literature, the selection of an IDM mainly depends on the RES technology, that is, whether it is synchronous generator or inverter based, since the dynamic behaviors of a synchronous generator-based RES are different from inverter-based RES after utility disconnection. The frequency of synchronous generator-based RES changes after utility disconnection even at exact power match conditions due to its mechanical inertia. Therefore, ROCOF is the most sensitive parameter utilized for islanding detection. Again, utility disconnection for synchronous generator-based RES can be easily detected using passive methods even at small power mismatch conditions [24]. Thus, the methods utilizing the ROCOF factor also has non-zero non-detection zone. However, this non-detection zone issue with PDMs can be solved by combining them with signal processing techniques. Therefore, a passive parameter is proposed, which is then analyzed using Wavelet transform. These issues have been considered in this paper and the following are the major contributions of the paper,

- Here, an IDM for a synchronous generator-based RES is proposed using the sequence components of the RES terminal voltage.
- A rate of change of voltage unbalance factor is computed from sequence components and this is analyzed using wavelet analysis for threshold setting. The factor is computed for discriminating all probable islanding scenarios from non-islanding scenarios.
- The proposed method can identify islanding events efficiently even at an exact power match condition, meaning it has a zero non-detection zone.
- The proposed method is also applicable to a multi-source system.

The content of the paper is organized as follows. Section 2 describes the proposed method along with a brief overview of the proposed parameter and wavelet transform concept. In Section 3, the simulation results for all the test systems in all probable islanding and non-islanding events are elaborated. A comparative analysis of the results for single source and multi-source system are discussed in Section 4, and conclusions of the research are presented in Section 5.

2. Test systems

The proposed method is tested in two sample test systems from [6]. One system is a single

source system and the other is a multi-source system.

2.1. Single source system

The test system has been simulated in MATLAB/Simulink. The single line diagram of single-source network is shown in Figure 1. A sub-transmission system of 132 kV, 60 Hz with a short-circuit level of 1500 MVA feeds a 33 kV distribution network through a 132/33 kV transformer. A synchronous generator of 30 MW is connected at bus 5 through a 33/0.69 kV transformer. The generator representing the RES is equipped with a voltage regulator. The system data is provided in Table 1. The rest system data are taken from [6].

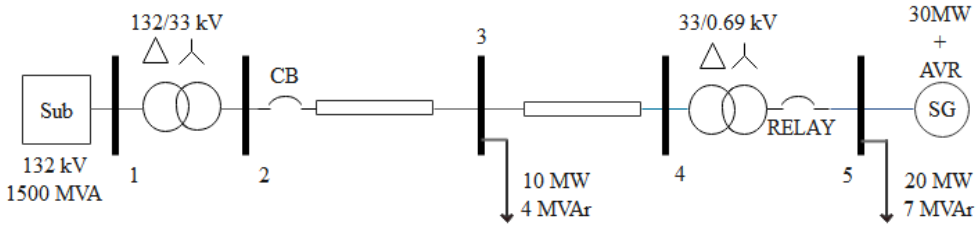

Figure 1. Single source test system [6].

Table 1. Single source test system data [6].

Sub-station	Voltage	132 kV
	Frequency	60 Hz
	SCC	1500 MVA
	R	0 ohm
	L	30.80 mH
Transformers	Delta/Star	100 MVA
		132/33 Kv
	R	0 pu
	L	0.04 pu
	Delta/Star	50 MVA
		33/0.69 kV
	R	0 pu
	L	0.04 pu
Line 2-3 (1 km)	R	0.37 (ohm/km)
	Xl	1.57 (ohm/km)
Line 3-4 (0.5 km)	R	0.97 (ohm/km)
	Xl	4.18 (ohm/km)
Loads	Rating	10 MW, 4 MVAR
		20 MW, 7 MVAR

2.2. Multi-source system

The multi-source system is simulated in a Simulink environment [6]. The system diagram is shown in Figure 2. The system consists of 138 kV and a 60 Hz sub-transmission network of 1000 MVA short-circuit level. A 25 kV distribution network is fed by the sub-transmission network through a 138/25 kV transformer. Two synchronous generators of 4.5 and 6 MW, respectively, are connected at bus 7 and 9 respectively to the distribution network through two 25/2.4 kV transformers. Two exciter systems controlled by voltage are provided to both the generators.

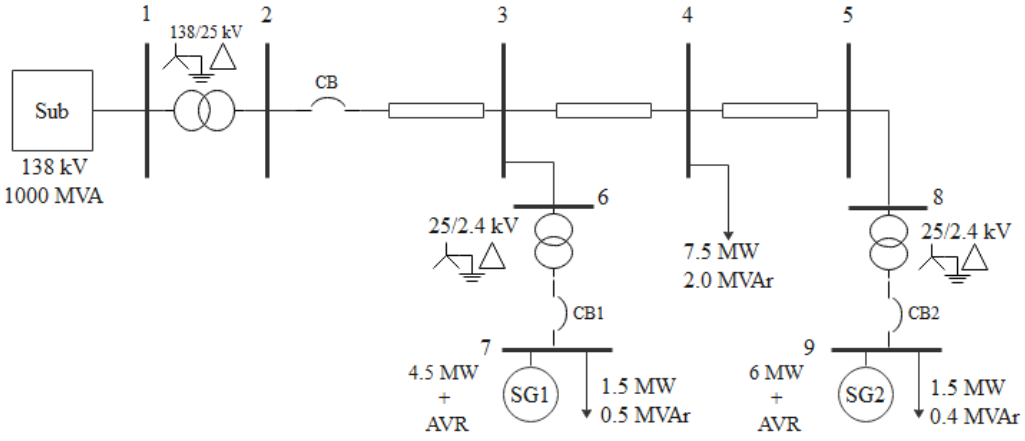

Figure 2. Single line diagram of a multi-source test system [6].

3. Proposed islanding detection method

In order to solve the non-detection issue in PDM, a new parameter is selected and wavelet analysis is also included in this paper. When islanding occurs in almost power match condition, the conventional PDM parameters sometimes fail to exceed the threshold value. However, the addition of wavelet transform will help to examine the minor variations in the selected parameter, thereby enabling the detection of utility disconnection even without adding any disturbance to the system. Here, the symmetrical components of the RES terminal voltage are calculated. The voltage unbalance factor is then found, and the rate of change of this voltage unbalance factor is used for generating the islanding detection signal along with the wavelet transform. The standard deviations for the detailed coefficients of the rate of change of the voltage unbalance (ROCOVU) parameter are used for discriminating the islanding conditions from non-islanding disturbances. The definition of the rate of change of voltage unbalance factor, a brief overview of wavelet transform, and the steps of the proposed method are explained as follows.

3.1. Rate of change of the voltage unbalance factor

As per the definition provided by IEC (International Electrotechnical Commission), the definition of the voltage unbalance factor is the ratio between negative and positive sequence voltages. Accordingly, the true voltage unbalance factor is mathematically expressed as [3],

$$VU = \frac{V_n}{V_p} \tag{1}$$

The positive and negative sequence components are expressed as,

$$V_p = \frac{V_{ab} + a \cdot V_{bc} + a^2 \cdot V_{ca}}{3} \tag{2}$$

$$V_n = \frac{V_{ab} + a^2 \cdot V_{bc} + a \cdot V_{ca}}{3} \tag{3}$$

where, $a = 1\angle 120^{\circ}$ and $a^2 = 1\angle 240^{\circ}$ [3]. In the proposed method, the rate of change of voltage unbalance (ROCOVU) is computed, using the following equations,

$$ROCOVU = \left|\frac{d(VU)}{dt}\right| \tag{4}$$

3.2. Wavelet transform

The Wavelet transform (WT) is a signal processing technique that is used for extracting features from the signals that change over time [15]. One of the advantages of using WT is its ability to remove noise from the signals. It is a class of functions expressing a signal in the time-frequency domain by decomposing it into its constituents at different frequency bands (or levels) known as wavelet coefficients [16]. WT has been used in many ways until now, so a brief overview is presented here. There are mostly two types of WT: Continuous WT (CWT) and discrete WT (DWT).

However, the DWT is extensively used due to its simplicity for implementation in digital signal processing (DSP), non-redundancy, and data compression capability, as well as computational efficiency [17,29]. DWT of a discrete signal x(n) is defined as,

$$DWT(m,k) = \frac{1}{\sqrt{a_0^m}} \sum_n x(n) \psi\left(\frac{k - n b_0 a_0^m}{a_0^m}\right) \tag{5}$$

where $\psi(..)$ is the mother wavelet, $a_0 > 1$ and $b_0 > 0$ are fixed real values, m and k positive integers that indicate frequency and time localization, respectively. The output of DWT is known as multi-resolution decomposition of the signal $x(n)$ with down-sampling. DWT decomposes signals into sub-bands, where the bandwidth increases linearly with frequency. Here, successive filtering of a signal is done using a series of low-pass filters and their corresponding high pass filters, in addition to down sampling. Thus,, $x(n)$ can be represented as,

$$x(n) = a_j(n) + \sum_{j=1}^{L} d_j(n) \tag{6}$$

where, a_j represent approximate coefficients, d_j represent detailed coefficients, and L is the maximum level of decomposition. The performance of the DWT analysis depends on the selection of a mother wavelet. The mother wavelet should be chosen based on the similarity between the signal to be analyzed and available mother wavelets.

After performing the simulations, Daubechies is found to be the appropriate mother wavelet, which is also least affected by noise. In this work, the Daubechies db5 wavelet with 9 levels is used with sampling frequency of 400 kHz. The standard deviation in the detail coefficient at level 2, which is d2, is used here for threshold setting in order to discriminate the islanding from other possible non-islanding disturbances. The steps of the proposed method are as follows:

Step1: take sampled values of measured three phase voltage from RES terminal

Step2: calculate the sequence components

Step3: find voltage unbalance factor

Step4: find the rate of change of voltage unbalance (ROCOVU) factor

Step5: find wavelet transform of ROCOVU

Step6: find standard deviation of 2^{nd} level detail coefficient

Step7: check standard deviation for threshold violation. If there is violation, islanding is detected and if there is no violation go to step 6.

Once islanding is detected, the trip signal is sent to the breaker, which connects the RES with the grid, in order to disconnect the RES from the grid so that the locally connected equipment and loads are protected from the uncontrolled islanded RES.

4. Results of simulation

Various islanding as well as non-islanding conditions are simulated in the two test systems. In order to evaluate the performance of the proposed method for non-detection zone, the system is simulated for different power mismatches in islanded condition. Robustness of the proposed method is also evaluated under several non-islanding conditions listed in Table 2. All possible conditions considered and the corresponding results are presented in succeeding sections.

Table 2. Possible system conditions

Islanding condition	For active power mismatch from 0% to 80%
	For both active power and reactive power mismatch from 0% to 80%
	With non-linear loads
Non-islanding condition	Single line to ground fault
	Double line to ground fault
	Double line fault
	Triple line to ground fault
	Triple line fault
	Inductive load switching

4.1. For single source system

Utility disconnection is simulated at 2 sec by opening the circuit breaker between utility and the RES with load of Figure 1. All the cases from Table 2 are simulated and presented for the test system afterwards.

4.1.1. Islanding condition with active power mismatches

For simulating active power mismatches, the active load on the system is varied from 20% to 100%, which is equivalent to 80% to 0% active power mismatch at 0% reactive power mismatch. The ROCOVU variation for some active power mismatches is shown in Figure 2 for clarity. From Figure 3, the variation of ROCOVU for small power mismatches clearly shows the sensitivity of the

proposed parameter. The standard deviation of d2 of ROCOVU for various power mismatches during islanding is given in Table 3.

4.1.2. Islanding condition with active and reactive power mismatches

In a similar manner, both active and reactive power loading are also varied and the variations are shown in Figure 4. Even for a wide range of both power variation, the ROCOVU factor shows considerable fluctuations throughout. The standard deviations for d2 of ROCOVU are given in Table 4.

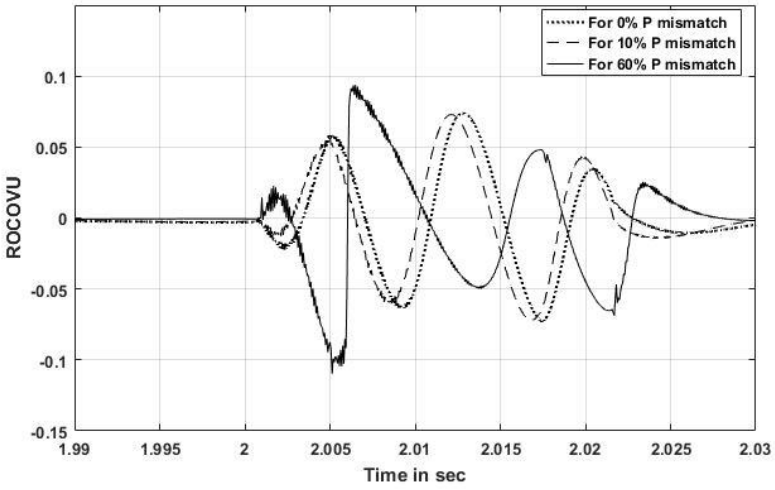

Figure 3. ROCOVU for 0%, 10%, and 60% active power mismatch.

Table 3. Standard deviation of d2 for islanding conditions with P mismatch.

Islanding condition	
P mismatch	Standard deviation of d2
80%	0.4433
70%	0.4960
60%	0.6335
50%	0.8080
40%	0.9852
30%	1.1557
20%	1.3191
15%	1.3987
10 %	1.4772
5%	1.5547
0%	1.6314

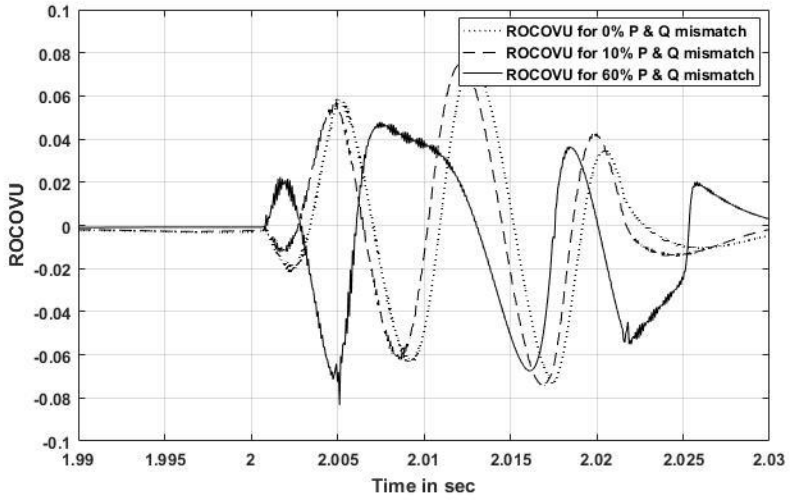

Figure 4. ROCOVU for 0%, 10%, and 60% active and reactive power mismatch.

4.1.3. Islanding condition with dynamic load

The variation of the ROCOVU parameter is also verified with a dynamic load from the Simulink library. The Three-Phase Dynamic Load block implements a three-phase, three-wire dynamic load whose active power P and reactive power Q vary as a function of positive-sequence voltage. The load impedance is kept constant if the terminal voltage V of the load is lower than a specified value V_{min} (set at 0.7 V). When the terminal voltage is greater than the V_{min} value, the active power P and reactive power Q of the load vary as follows:

$$P(s) = P_0 \left(\frac{V}{V_0}\right)^{n_p} \frac{1+T_{p1}s}{1+T_{p2}s} \tag{7}$$

$$Q(s) = Q_0 \left(\frac{V}{V_0}\right)^{n_q} \frac{1+T_{q1}s}{1+T_{q2}s} \tag{8}$$

where, V_0 is the initial positive sequence voltage, P_0 and Q_o are the initial active and reactive powers at the initial voltage V_o, V is the positive-sequence voltage, n_p and n_q are the exponents (usually between 1 and 3) controlling the nature of the load, T_{p1} and T_{p2} are time constants controlling the dynamics of the active power P, T_{q1}, and T_{q2} are the time constants controlling the dynamics of the reactive power Q.

The dynamic load is connected to the single source test system and then utility is disconnected at 2 sec. Even at 0% power mismatch there is no effect of dynamic load on the ROCOVU parameter as shown in Figure 5. The corresponding standard deviation is tabulated in Table 4.

4.1.4. Non-islanding conditions

For the non-islanding conditions inductive load switching, capacitive load switching is simulated. A total of 100 MVAR inductive and capacitive loads are switched in two separate cases at 1.5 sec to the system. Figure 6 shows a comparison of the capacitive load switching and islanding at 0% power mismatch. It shows that the amplitude variation in load switching is much more than the utility disconnection case. The corresponding standard deviation in d2 for the two-load switching are given in Table 5.

Moreover, all possible fault cases are also simulated. The fault is initiated at 1.5 sec and is cleared after four cycles in the single source test system for all fault cases. A comparison of the most common single line to ground fault with the islanding condition at 0% power mismatch is shown in Figure 7. Standard deviation for all possible faults are also given in Table 5.

Table 4. Standard deviation of d2 for islanding condition for both P and Q mismatch and for dynamic load.

Islanding condition	
P and Q mismatch	Standard deviation of d2
80%	0.4703
70%	0.6512
60%	0.6514
50%	0.8260
40%	1.0016
30%	1.1690
20%	1.3284
15%	1.4059
10 %	1.4821
5%	1.5572
0%	1.5701
With dynamic load	1.3964

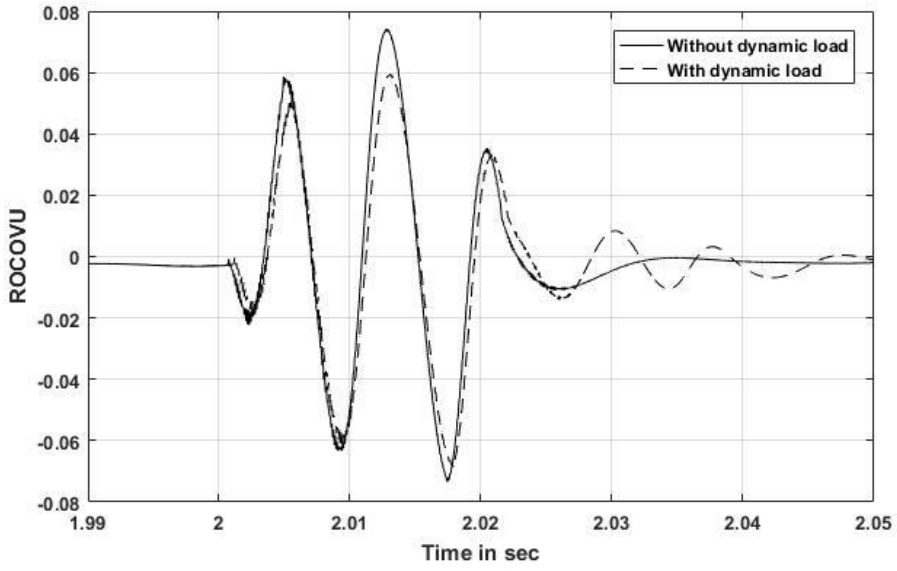

Figure 5. ROCOVU with and without dynamic load at 0% power mismatch.

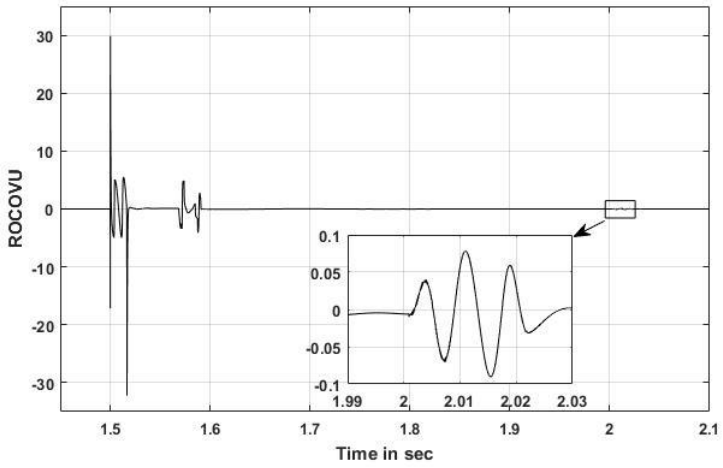

Figure 6. ROCOVU for capacitive load switching and islanding condition (load switching at 1.5 sec and islanding inception at 2 sec).

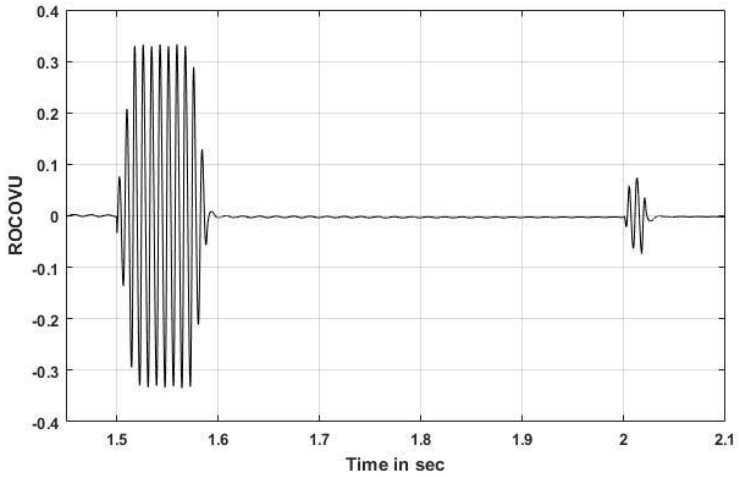

Figure 7. ROCOVU for single line to ground fault and islanding condition (fault inception at 1.5 sec and islanding inception at 2 sec).

Table 5. Standard deviation for non-islanding conditions.

Non-islanding condition	
Load switching	Standard deviation of d2
L load	1.6425
C load	1.6566
Faults	
LLL	1.6318
LLLG	1.6318
LL	1.6318
LLG	1.6318
LG	1.6318

4.2. For multi-source system

In this test system, islanding is simulated by disconnecting circuit breaker CB shown in Figure 2 at 1.7 sec. The results for all possible conditions from Table 2 are presented as follows.

4.2.1. Islanding conditions for active power mismatches

The islanding conditions for all active mismatches are simulated. Then, the standard deviations of d2 of ROCOVU are also computed for both RES. Variation of ROCOVU for active power mismatches are shown in Figures 8 and 9 for SG1 and SG2. Here, also Daubechies is considered as a mother wavelet, and d2 is utilized. The standard deviation in wavelet coefficients for ROCOVU for active power mismatches is given in Table 6 (a) and (b) for both RESs.

4.2.2. Islanding conditions for active and reactive power mismatches

The islanding conditions for both active and reactive power mismatches are simulated. Then, the standard deviations of d2 of ROCOVU are also computed for both RESs. Variation of ROCOVU for some active and reactive power mismatches are shown in Figures 10 and 11 for SG1 and SG2. The standard deviation in wavelet coefficients for ROCOVU for both active and reactive power mismatches and for dynamic loading is given in Table 7 (a) and (b) for both RESs.

4.2.3. Non-islanding conditions

Different non-islanding scenarios are created by adding inductive and capacitive loads and by initiating various symmetrical and asymmetrical faults as before. Such non-islanding scenarios must go undetected by the method. The proposed ROCOVU parameter for the passive method is shown for some selected non-islanding scenarios in Figures 12 and 13 for SG1. These figures show that there is a very small effect of load switching and faults on ROCOVU of SG1. It is seen that ROCOVU of SG2 remain unaffected in both non- islanding scenarios. Again, wavelet transform of all the above ROCOVU variations are performed and the standard deviations for d2 are tabulated in Table 8 (a) and (b).

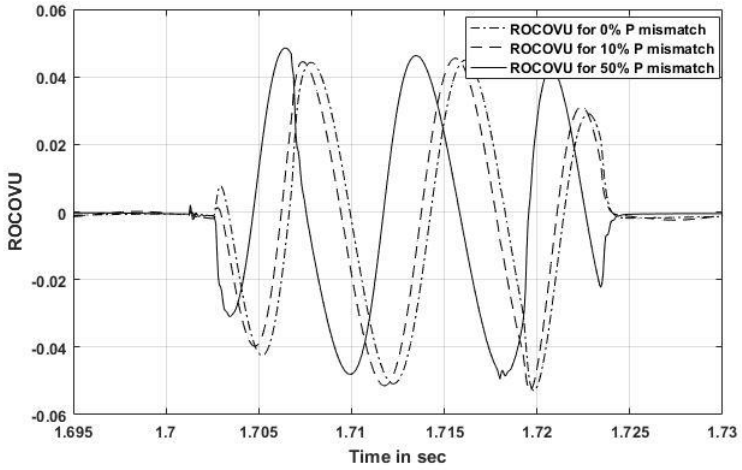

Figure 8. ROCOVU for 0%, 10% and 50% P mismatch for SG1.

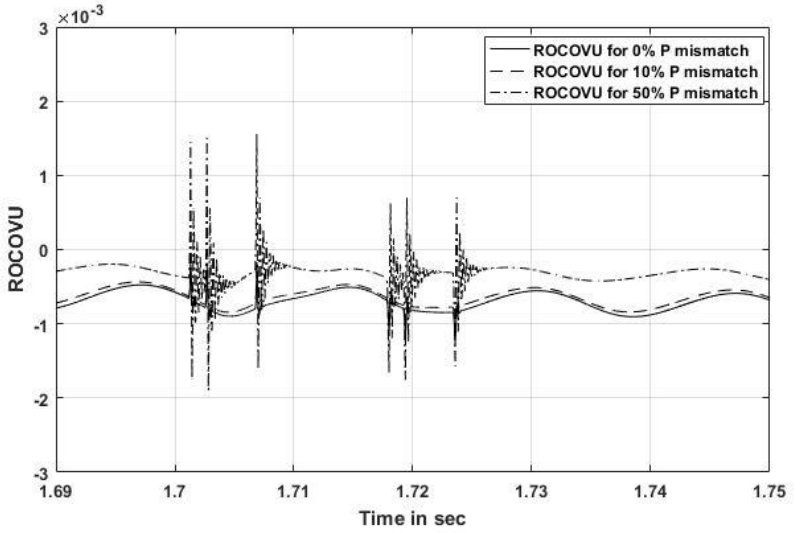

Figure 9. ROCOVU for 0%, 10% and 50% P mismatch for SG2.

Table 6. Standard deviation of d2 for islanding conditions (a) for SG1 and (b) for SG2.

(a)

Islanding condition for SG1	
P mismatch	Standard deviation of d2
50%	0.4569
40%	0.5133
30%	0.5729
20%	0.6524
15%	0.6968
10 %	0.7429
5%	0.7901
0%	0.8378

(b)

Islanding condition for SG2	
P mismatch	Standard deviation of d2
50%	0.4613
40%	0.4237
30%	0.4634
20%	0.5044
15%	0.5239
10 %	0.5467
5%	0.5729
0%	0.6018

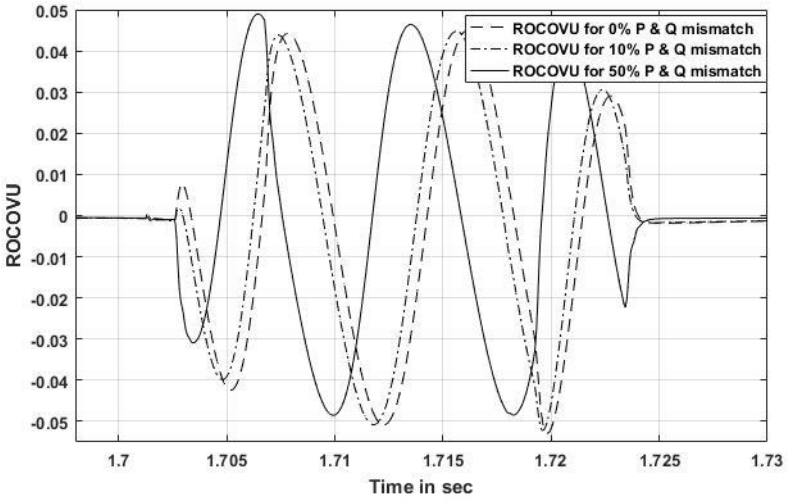

Figure 10. ROCOVU for 0%, 10% and 50% P and Q mismatch for SG1.

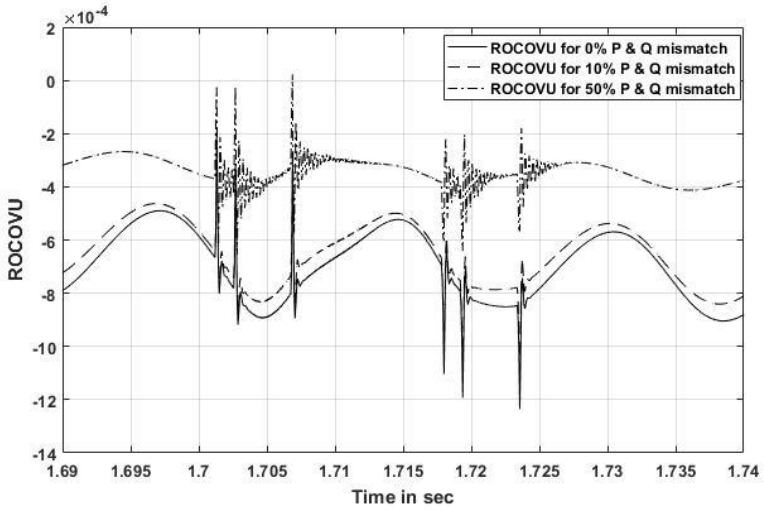

Figure 11. ROCOVU for 0%, 10% and 50% P and Q mismatch for SG2.

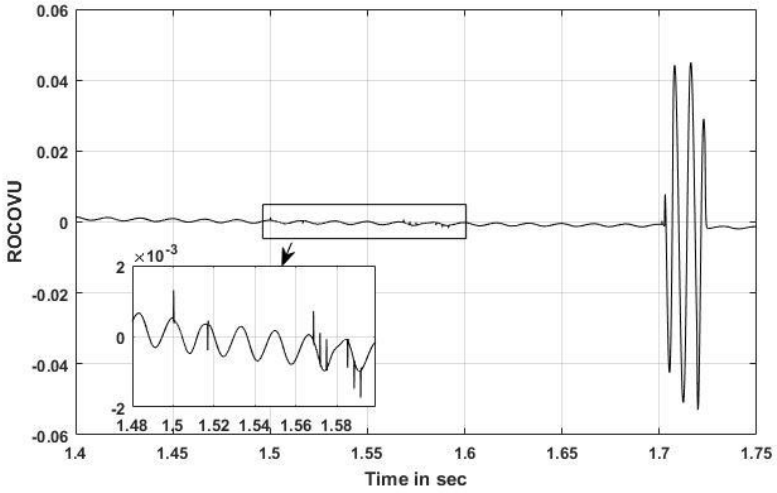

Figure 12. ROCOVU for capacitive load switching at 1.5 sec and islanding inception at 1.7 sec in SG1.

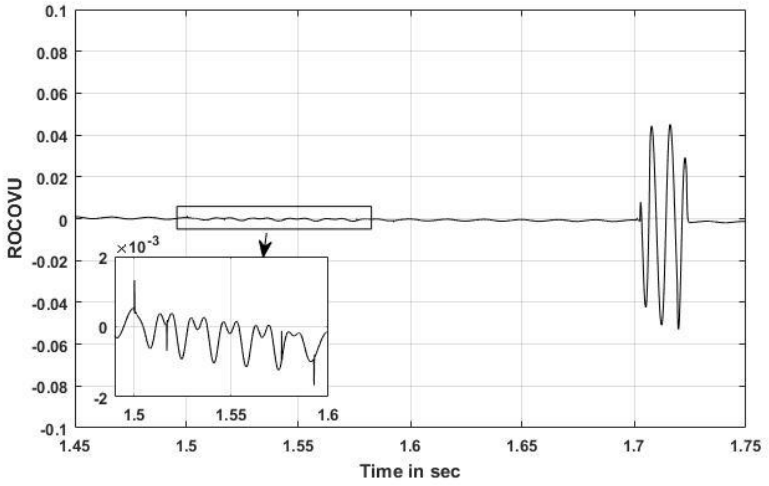

Figure 13. ROCOVU for fault at 1.5 sec and islanding inception at 1.7 sec in SG1.

Table 7. Standard deviation of d2 for islanding conditions (a) for SG1 and (b) for SG2.

(a)

Islanding condition for SG1	
PQ mismatch	Standard deviation of d2
50%	0.4558
40%	0.5124
30%	0.5724
20%	0.6525
15%	0.6970
10 %	0.7432
5%	0.7903
0%	0.8378
With dynamic load	0.7982

(b)

Islanding condition for SG2	
PQ mismatch	Standard deviation of d2
50%	0.4559
40%	0.4216
30%	0.4617
20%	0.5035
15%	0.5233
10 %	0.5463
5%	0.5727
0%	0.6018
With dynamic load	0.5903

Table 8. Standard deviation for non-islanding conditions (a) for SG1 and (b) for SG2.

(a)

Non-islanding condition	
Load switching	Standard deviation of d2
L load	0.8380
C load	0.8380
Faults	
LLL	0.8380
LLLG	0.8380
LL	0.8380
LLG	0.8380
LG	0.8380

(b)

Non-islanding condition	
Load switching	Standard deviation of d2
L load	0.6020
C load	0.6020
Faults	
LLL	0.6020
LLLG	0.6020
LL	0.6020
LLG	0.6020
LG	0.6020

4.3. Performance comparison with other methods

Many IDMs are applicable only to inverter interfaced RESs. Only a few are applicable to both inverter based and SG based RESs. A ROCOF based PDM is one of the oldest and proven methods of protection for SG based RESs. In [6], it is verified that the ROCOF relay can detect utility disconnection for power imbalances at more than 15%. In Figure 14, both ROCOVU and ROCOF are plotted for 0% power mismatch.

On comparing the proposed method with the conventional ROCOF method used for synchronous generator-based RESs, from Figure 14, it is clear that the ROCOF method-based relays fail to operate at lower values of power mismatches, whereas the proposed method can operate faster and more reliably even at exact power balances between grid and the local load, which corresponds to 0% power mismatch.

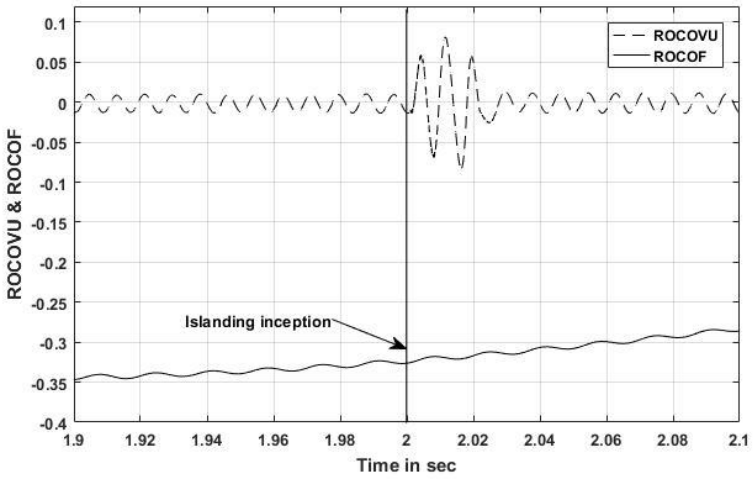

Figure 14. ROCOVU and ROCOF for 0% power mismatch.

A comparison of performance of the proposed method with other hybrid IDMs is given in Table 9. From the table, we can see that the proposed method does not affect the power quality and is applicable to multi-source systems with zero NDZ.

Table 9. Comparison with other hybrid methods for synchronous generator-based RES.

Methods	NDZ	Power quality	Applicability to Multi-source system
Paiva et.al. [22]	Small NDZ	Small effect	Applicable
Menon et.al. [25]	No information	Small effect	Applicable
Chang [26]	No information	Small effect	Not applicable
Pouryekta et.al. [27]	No information	Small effect	Applicable
Singh et.al. [28]	Small NDZ	No effect	No information
Proposed method	Zero NDZ	No effect	Applicable

5. Discussion

Islanding conditions with various power mismatches and for dynamic loading are considered here for both single source and multi-source system. From Tables 3 and 4, the standard deviation can be seen to reduce from 1.6314 (standard deviation value for 0% mismatch) for all other power mismatches. Tables 3 to 5 clearly show that the standard deviation values for non-islanding conditions are more than 1.6314, which is the maximum for all islanding conditions and corresponds to 0% power mismatch. Thus, 1.6314 can be considered as the threshold value for discriminating the islanding and non-islanding conditions for the single source system. The average detection time for this single source system is found to be 0.024430 sec after inception of utility disconnection. Thus, the detection time is also in accordance with the IEEE 1547 standard.

For a multi-source system, Table 8 shows that the standard deviation is constant for all non-islanding conditions. This shows the strength of the proposed method to remain unaffected by non-islanding scenarios. On comparing Tables 6 to 8, we can take 0.8378 and 0.6018 as the

thresholds, which correspond to 0% power mismatch in both active and apparent power for SG1 and SG2, respectively. Thus, the proposed wavelet transform based passive method is very much effective and highly reliable with a range of power mismatches. The response even at lower mismatches is proof for the zero non-detection zone. Again, the average time taken for the detection of islanding for this multi-source system is 0.027961 sec after the inception of islanding. Thus, the detection time is well within the IEEE 1547 requirements. Again, from the performance comparison with other methods, we can see that the proposed method can be used for systems with multiple sources without affecting the system power quality even at exact power match conditions, unlike ADM.

6. Conclusions

Here, a hybrid IDM is proposed using a new passive parameter based on sequence components. The use of proposed passive parameters helps in reducing the non-detection zone to zero. The proposed hybrid IDM is found to operate even for small power mismatches, where usually the conventional passive methods like ROCOF method fails. Specifically, we focused on testing the performance of the proposed method for very small values of power mismatches as low as 0%. Again, the issue of threshold setting is tackled by wavelet transform. The analysis of the ROCOVU factor using wavelet transform helped in the setting of the threshold, so that any nuisance tripping during non-islanding conditions could be avoided. The performance of the proposed method is also tested for a wide range of operating conditions, including the multi-source system. Again, comparison of the proposed method with other hybrid methods also proved its reliability. Thus, the method is faster, more reliable, and is easy to implement in real-time microgrids. In future work, the proposed parameter can be used in any of the IDMs for improving the performance of existing ADMs, RDMs, and HDMs.

Use of AI tools declaration

The authors declare that they have not used Artificial Intelligence (AI) tools in the creation of this article.

Conflict of interest

All authors declare no conflicts of interest in this paper.

References

1. IEEE Standard for Interconnecting Distributed Resources with Electric Power Systems (2003) IEEE Standard 1547-2003.
2. Khamis A, Shareef H, Bizkevelci E, Khatib T (2013) A review of islanding detection techniques for renewable distributed generation systems. *Renew Sust Energ Rev* 28: 483–493. https://doi.org/10.1016/j.rser.2013.08.025
3. Li C, Cao C, Cao Y, Kuang Y, Zeng L, Fang B (2014) A review of islanding detection methods for microgrid. *Renew Sust Energ Rev* 35: 211–220. https://doi.org/10.1016/j.rser.2014.04.026

4. Velasco D, Trujillo CL, Garcera G, Figueres E (2010) Review of anti-islanding techniques in distributed generators. *Renew Sust Energ Rev* 14: 1608–1614. https://doi.org/10.1016/j.rser.2010.02.011
5. Mishra M, Chandak S, Rout PK (2019) Taxonomy of Islanding detection techniques for distributed generation in microgrid. *Renew Energ Focus* 31: 9–30. https://doi.org/10.1016/j.ref.2019.09.001
6. Freitas W, Xu W, Affonso CM, Huang Z (2005) Comparative analysis between ROCOF and vector surge relays for distributed generation applications. *IEEE T Power Del* 20: 1315–1324. https://doi.org/10.1109/TPWRD.2004.834869
7. Liu F, Kang Y, Zhang D, Y. S., and Lin X (2010)Improved SMS islanding detection method for grid-connected converter. *IET Renew Power Gen* 4: 36–42. https://doi.org/10.1049/iet-rpg.2009.0019
8. Zeineldin HH, Salama MMA (2011) Impact of load frequency dependence on the NDZ and performance of the SFS islanding detection method. *IEEE T Ind Electron* 58: 139–146. https://doi.org/10.1109/TIE.2009.2033482
9. Velasco D, Trujillo C, Garcera G, Figueres E (2011) An active anti-islanding method based on phase-PLL perturbation. *IEEE T Power Electron* 26: 1056–1066. https://doi.org/10.1109/TPEL.2010.2089643
10. Papadimitriou CN, Kleftakis VA, Hatziargyriou ND (2015) A novel islanding detection method for microgrids based on variable impedance insertion. *Electr Power Syst Res* 121: 58–66. https://doi.org/10.1016/j.epsr.2014.12.004
11. Seyedi M, Taher SA, Ganji B, Guerrero JM (2019) A hybrid islanding detection technique for inverter-based distributed generator units. *Int Trans Electr Energ Syst* 29: e12113. https://doi.org/10.1002/2050-7038.12113
12. Pouryekta A, Ramachandaramurthy VK, Mithulananthan N, Arulampalam A (2018) Islanding Detection and Enhancement of Microgrid Performance. *IEEE Syst J* 12: 3131–3141. https://doi.org/10.1109/JSYST.2017.2705738
13. Raza S, Mokhlis H, Arof H, Laghari JA, Wang L (2015) Application of signal processing techniques for islanding detection of distributed generation in distribution network: A review. *Energ Convers Manage* 96: 613–624. https://doi.org/10.1016/j.enconman.2015.03.029
14. Hussain A, Kim CH, Mehdi A (2021) A Comprehensive Review of Intelligent Islanding Schemes and Feature Selection Techniques for Distributed Generation System. *IEEE Access* 9: 146603–146624. https://doi.org/10.1109/ACCESS.2021.3123382
15. Avdakovic S, Nuhanovic A, Kusljugic M, Music M (2012) Wavelet transform applications in power system dynamics. *Electr Power Syst Res* 83: 237–245. https://doi.org/10.1016/j.epsr.2010.11.031
16. Dwivedi UD, Singh SN (2010) Enhanced detection of power-quality events using intra and interscale dependencies of wavelet coefficients. *IEEE T Power Deliver* 25: 358–366. https://doi.org/10.1109/TPWRD.2009.2027482
17. Laaksonen H (2013) Novel wavelet transform based islanding detection algorithms. *Int Rev Electr Eng* 8: 1796–1805.
18. Hanif M, Dwivedi UD, Basu M, Gaughan K (2010) Wavelet based islanding detection of DC–AC inverter interfaced DG systems. *45th international universities power engineering conference (UPEC)*, 1–5.

19. Karegar HK, Sobhani B (2012) Wavelet transform method for islanding detection of wind turbines. *Renew Energy* 38: 94–106. https://doi.org/10.1016/j.renene.2011.07.002
20. Hanif M, Basu M, Gaughan K (2012) Development of EN50438 compliant wavelet-based islanding detection technique for three-phase static distributed generation systems. *IET Renew Power Gen* 6: 289–301. https://doi.org/10.1049/iet-rpg.2011.0290
21. Sharma R, Singh P (2012) Islanding detection and control in grid based system using wavelet transform. *5th IEEE power india conference*, 1–4. https://doi.org/10.1109/PowerI.2012.6479557
22. Paiva SC, Ribeiro RLA, Alves DK, Costa FB, Rocha TOA (2020) A wavelet-based hybrid islanding detection system applied for distributed generators interconnected to AC microgrids. *Int J Electr Power Energ Syst* 121: 106032. https://doi.org/10.1016/j.ijepes.2020.106032
23. Nsaif YM, Lipu MSH, Ayob A, Yusof Y, Hussain A (2021) Fault Detection and Protection Schemes for Distributed Generation Integrated to Distribution Network: Challenges and Suggestions. *IEEE Access* 9: 142693–142717, https://doi.org/10.1109/ACCESS.2021.3121087
24. Bekhradian R, Sanaye-Pasand M (2022) A Comprehensive Survey on Islanding Detection Methods of Synchronous Generator-Based Microgrids: Issues, Solutions and Future Works. *IEEE Access* 10: 76202–76219, https://doi.org/10.1109/ACCESS.2022.3192554
25. Menon V, Nehrir MH (2007) A Hybrid Islanding Detection Technique Using Voltage Unbalance and Frequency Set Point. *IEEE T Power Syst* 22: 442–448. https://doi.org/10.1109/TPWRS.2006.887892
26. Chang WY (2010) A hybrid islanding detection method for distributed synchronous generators. *The 2010 International Power Electronics Conference - ECCE ASIA -*, 1326–1330. https://doi.org/10.1109/IPEC.2010.5544559
27. Pouryekta A, Ramachandaramurthy VK (2018) A Hybrid Islanding Detection Method For Distribution Systems. *Distributed Generation & Alternative Energy Journal* 33: 44–67. https://doi.org/10.1080/21563306.2018.12029914
28. Singh SK, Rawal M, Rawat MS, Gupta TN (2022) A Hybrid Islanding Detection Technique for Synchronous Generator Based Microgrids. *Power Electronics and High Voltage in Smart Grid: Select Proceedings of SGESC 2021*, 365–374. https://doi.org/10.1007/978-981-16-7393-1_31
29. Larik NA, Tahir MF, Elbarbary ZMS, Yousaf MZ, Khan MA (2022) A comprehensive literature review of conventional and modern islanding detection methods. *Energy Strategy Rev* 44: 101007. https://doi.org/10.1016/j.esr.2022.101007

AIMS Press